Global and Planetary Change 236 (2024) 104411

Contents lists available at ScienceDirect

Global and Planetary Change

journal homepage: www.elsevier.com/locate/gloplacha

Historical catastrophic floods at the southern edge of the Atacama Desert: A multi-archive reconstruction of the Copiapó river extreme events

Tatiana Izquierdo [a,b,*], Ai-ling Rivera [a], Ángela Galeano [a], Diego Gallardo [c], Verónica Salas [a], Olga Aparicio [a], Jan-Pieter Buylaert [d], Francisco Ruiz [e], Manuel Abad [a,b]

[a] Research Group in Earth Dynamics and Landscape Evolution (DYNAMICAL), Universidad Rey Juan Carlos, Móstoles, Spain
[b] Department of Biology and Geology, Physics and Inorganic Chemistry, Universidad Rey Juan Carlos, Móstoles, Spain
[c] Departament of Statistics, Bío-Bío University, Concepción, Chile
[d] Department of Physics, Technical University of Denmark, DTU Risø campus, Roskilde, Denmark
[e] Department of Earth Sciences, Universidad de Huelva, Spain

ARTICLE INFO

Editor: Dr. Jed O Kaplan

Keywords:
Historical floods
Palaeohydrology
Flood frequency analysis
Copiapó River
Atacama

ABSTRACT

The last hydrometeorological extreme event that caused large floods in the southern Atacama Desert in March 2015 raised concern about how little was known about the fluvial dynamic of these arid basins. Understanding the response of intermittent and ephemeral rivers in drylands to the present context of global change is critical to preserve the ecological and human systems they support, to sustainably manage their scarce water resources and to develop flood risk management plans. We have studied the instrumental and historical record and explored the potential of the Copiapó River geological record in the comprehension of how extraordinary the 2015 flood was and how its fluvial dynamic relates with global climate oscillations. We have identified 36 flood events that have occurred in the last 400 years: 22 of them have been classified as ordinary rises of the river flow (discharges <30 m^3/s), 11 as extraordinary floods in which the damage is confined to areas adjacent to the river (discharges 30–180 m^3/s), and only 3 as catastrophic floods (discharges >180 m^3/s), including the 2015 flood event. The incorporation of the historical and palaeohydrological data into the flood frequency analysis results in an increase of the magnitude of the flood quantiles in which large flood events occur with an average recurrence interval of 120 years. Most of the flood events were caused by heavy rains that are largely linked to the Pacific Decadal Oscillation and the Atlantic Multidecadal Oscillation with a superimposed effect of the ENSO. Discharges >30 m^3/s, i.e., extraordinary and catastrophic floods, occur with positive phases of the PDO and the ENSO. Further exploration of the fluvial geological record of the Copiapó River will help lengthening to thousands of years the flood record what will help improving communities' resilience by anticipating flood hazards in the current global change context, in which stronger rainfall events modulated by ENSO and ENSO-like conditions are expected.

1. Introduction

Intermittent and ephemeral rivers are formed in drylands, where aridity and climate variability are the most important natural factors defining the fluvial dynamic (Botes et al., 2003). In the present context of global change (IPCC, 2023), understanding their response to global warming is critical to preserve the ecological and human systems they support (Botes et al., 2003), to sustainably manage their scarce water resources (Morin et al., 2009) and to develop flood risk management plans (Milly et al., 2002). Despite its importance, hydrological response to climate change is one of the major uncertainties of future climate scenarios due to the complexities associated, particularly in arid regions where the lack of monitoring station networks and thus, instrumental records add uncertainty (Schick, 1988).

Fluvial systems in drylands are then sporadically activated after intense storms, resulting in high-energy, short-term runoff that can cause flooding (Grodek et al., 2013). Historical records of this process are often used to supplement assessments of current and projected flood hazard (Wilhelm et al., 2019). Unfortunately, their temporal range, which is several millennia in some regions such as the Mediterranean, is

* Corresponding author at: Research Group in Earth Dynamics and Landscape Evolution (DYNAMICAL), Universidad Rey Juan Carlos, Móstoles, Spain.
E-mail address: tatiana.izquierdo@urjc.es (T. Izquierdo).

https://doi.org/10.1016/j.gloplacha.2024.104411
Received 19 June 2023; Received in revised form 14 January 2024; Accepted 6 March 2024
Available online 11 March 2024

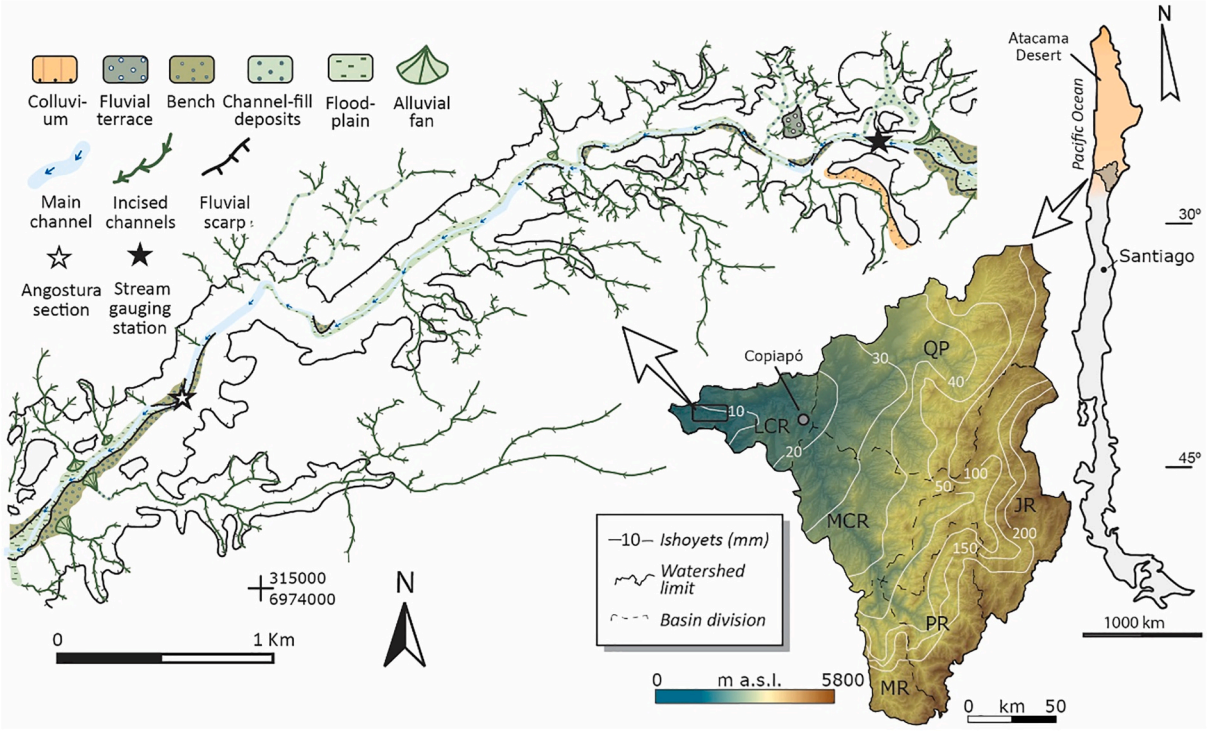

Fig. 1. Right: Location of the study area within Chile and the Atacama Desert. Center: The Copiapó River catchment showing the digital elevation model, subbasins division (QP: Quebrada Paipote; JR: Jorquera River; PR: Pulido River; MR: Manflas River; MCR: Middle Copiapó River; LCR: Lower Copiapó River) rainfall isohyets (DGA, 2010), location of the city of Copiapó and the Angostura canyon. Left: Geomorphological sketch map of the Angostura canyon and location of the Angostura stream gauging station and the stratigraphic profile containing flood deposits.

quite short in others such as South America (Wilhelm et al., 2019). On the other hand, these high-energy events are recorded in the fluvial sedimentary sequences and geoforms, so it is possible the use of geomorphological and sedimentological techniques to determine when and how these (paleo)floods occurred and to complement the historical and instrumental record (Baker, 2000). Benito et al. (2020a) provided an overview of the most common paleoflood depositional environments, which include areas of channel widening, obstacle hydraulic shadows where flow separation results in eddies, or back-flooded tributary mouths and valleys, and emphasized the importance of the geomorphological assessment of the study sites. Both types of non-systematic information complement the instrumental record with information on the largest floods of the past hundreds to thousands of years and can be used for both paleoclimatic interpretation and flood risk analysis (Benito et al., 2004; Schulte et al., 2019; Baker et al., 2022).

Understanding the patterns of extreme events in the context of global change is critical because of their social, political, and economic impacts, especially for regions where extremes are a key feature of their hydrologic system, such as (semi)arid regions (e.g., Benito et al., 2010; Benito et al., 2020b; Macklin et al., 2010; Miller et al., 2019; Liu et al., 2020; Cloete et al., 2018, 2022). This became evident after the last extreme hydrometeorological event that caused large floods in the southern Atacama Desert in March 2015 (Barrett et al., 2016; Bozkurt et al., 2016; Valdés-Pineda et al., 2018), when the Copiapó River had an exceptional peak discharge of 240 m^3/s, while the measured mean annual discharge is only 0.43 m^3/s (Izquierdo et al., 2020, 2021). In fact, during this event, the city of Copiapó was catastrophically affected as a muddy deposit buried >70% of the urban area and the economic activity in the affected sector was paralyzed for almost a month, which caused an estimated impact of >45 million USD (Observatorio Económico de Chile, 2015).

To understand how extraordinary the 2015 event was for the Copiapó fluvial system, we have explored the historical and geological archives to reconstruct the flood history of the last four centuries on this arid basin and its relationship with global climate. These results will help understanding the future behavior of these arid fluvial systems and the main factors controlling the occurrence of the next catastrophic flood.

2. Study area

The Copiapó River, flowing from east to west (Fig. 1), is considered the southern limit of the Atacama Desert (Navarro et al., 2021), because to the north rivers are ephemeral while to the south, they are perennial under natural conditions. This hydrologic boundary results from the end of the extreme arid conditions as a consequence of the current position of the so-called "South American Arid Diagonal" (De Martonne, 1935; Abraham et al., 2020), which crosses at the latitude of the Copiapó River (27°S). Here, the arid climate is controlled by the South Pacific High and the Humboldt Current, which prevent precipitation from the Pacific Ocean (Houston, 2006a). The low rainfall values vary latitudinally and altitudinally (Valdés-Pineda et al., 2014; Fig. 1) with a mean annual rainfall of 20.9 mm in the city of Copiapó. Traditionally, above-average rainfall values have been linked to El Niño conditions (Vargas et al., 2000; Vargas et al., 2006; Ortlieb and Vargas, 2015). However, Valdés-Pineda et al. (2018) have recently identified a low-frequency variability in precipitation that occurs at the latitude of Copiapó with a cycle that varies between 40 and 60 years and that is strongly influenced by the Pacific Decadal Oscillation index (PDO) and the Atlantic Multi-decadal Oscillation Index (AMO). In fact, according to these authors, the March 2015 event coincided with a high phase of the AMO index, implying a high amount of precipitable water at low latitudes, enhanced by the high seawater temperatures generated by the 2015–2016 ENSO phenomenon.

The city of Copiapó (~160,000 inhabitants) was established in 1744 although it was the first Chilean valley to be explored by Europeans in

1536 as they traveled south from Peru (Sayago, 1874). It is located in the alluvial plain of the Copiapó River, downstream of the junction between the Quebrada Paipote and the main valley (Fig. 1), i.e., exposed to periodic floods and mudflows throughout its history (e.g., Darwin, 1845; Sayago, 1874; Mackenna, 1877; Bowman, 1925) and during the Late Holocene (Izquierdo et al., 2017, 2019). The Copiapó watershed (18,400 km^2) can be divided into two major areas: (1) the Quebrada Paipote subbasin (6689 km^2) with an ephemeral behavior and (2) the Copiapó River valley (11,711 km^2) with an intermittent behavior and a mixed snowmelt and rain fed regime (Fig. 1). The river is currently highly regulated by a dam (40 Hm^3) in the upper catchment for agricultural and mining purposes. Its mean discharge at the city during the 1974–2005 time series was 2.4 m^3/s. Since 2005 the river has flowed dry through the city of Copiapó due to its overexploitation except during extraordinary events.

Near the river mouth and 50 km downstream the city, in the Angostura sector (Fig. 1), groundwater springs and the river become permanent again with an average discharge of 0.12 m^3/s. This spring is caused by the contact between the alluvial aquifer and the uplifted metamorphic Paleozoic and igneous Jurassic substratum (Godoy et al., 2003). The coastal uplift during the last 800 ky (Marquardt et al., 2004; Quezada et al., 2007) has made the river to erode a canyon >80 m deep in these geological materials (Fig. 1) that abruptly widens near the coast when the valley reaches the Neogene substrate. Thus, this site gathers two key features for a paleohydrologic study: (a) a bedrock-confined channel and (b) an area of channel widening at the exit of the canyon (Benito et al., 2003, 2020a).

3. Data sources and methods

3.1. Instrumental records

In order to accurately analyze the hydroclimatic variability in the study area it is required to obtain the longest existing time series. The Dirección General de Aguas (DGA; https://dga.mop.gob.cl) and the Dirección Meteorológica Chile (DMC; https://climatologia.meteochile.gob.cl) time series start in the late 1980s and were completed using the meteorological information available at the Yearbooks of the Meteorological Service of Chile (Department of Geophysics of the University of Chile; http://biblioteca.dgf.uchile.cl/anuarios/anuariosmeteorologicoschilenos.html) that began in the 19th century. In addition, these time series were completed with historical sources that include meteorological information (Sayago, 1874; Mackenna, 1877; Bowman, 1925; Almeyda, 1948). Although precipitation data exists since 1795, the period 1795–1887 correspond to annual and not monthly rainfall data and they cannot be used for calculating the climatic indices. During the 132 years studied (1888–2020), the official rain gauge had three different locations: Copiapó city (1888–1970); Copiapó Chamonate airport (1971–2005); and Atacama Desert airport (2006-present). Although monthly temperature records are available since 1856, the series was very incomplete and a shorter series of only 74 years (1946–2020) was used.

The series of average daily flows and maximum daily flows were obtained from the Dirección General de Aguas (DGA; https://dga.mop.gob.cl) for the City of Copiapó and Angostura gauges (1983–2020 and 1969–2020 respectively). A double mass analysis was used to complete the poorest data series. In addition, on many occasions extreme flood peak discharge data is estimated through indirect methods after the end of the event, due to the failure or destruction of the measuring stations in the process (Benito et al., 2004) as occurred in the study area during the extreme hydrometeorological event of March 2015 (Izquierdo et al., 2021). Thus, as no recorded peak discharge value exists for the 2015 flood, the discharge values modelled by the DOH (2016) were included in the flood frequency analysis.

3.2. Historical data sources

The historical period in Chile begins in 1536, when the first Spaniards arrived at the valley of Copiapó, following the Inca trail from Peru and crossing the Andes. Although it was the first Chilean valley explored by Europeans and it had been inhabited for thousands of years (Niemeyer et al., 1997; Falabella et al., 2017), the city of Copiapó was not founded until 1744, when it was named San Francisco de la Selva de Copiapó. Documentation for this first 200-year period is extremely scarce, with only a few 18th and 19th century chronicles describing years or periods of abundant rain and/or flooding (Philippi, 1860; Sayago, 1874; Mackenna, 1877; Bowman, 1925; Barreiro, 1929). Official archives have existed since the city's founding, and thus it is possible to access a broader range of records such as letters, financial and legal documents, which include local and regional government records located in the Copiapó Municipal Historical Archive and the Atacama regional Museum Archive. In addition, magazines and newspapers published periodically since the beginning of the 19th century were reviewed at the Chilean National Library to obtain additional information and detailed descriptions of the events that occurred more recently. Finally, we included in the analysis the last two events from 2015 and 2017 (Izquierdo et al., 2021). We classified the Copiapó River flood events in three categories by adjusting the methodology proposed by Barriendos et al. (2003) and assigning discharge perception thresholds: (1) Ordinary rise or small flood, meaning a small increase in flow is perceived and minor damages in irrigation in infrastructures occur; in the Copiapó River this occurs after heavy rains or snowmelt episodes; (2) Extraordinary flooding or intermediate flood, meaning the flooding is confined to areas adjacent to the river where it causes damage to railway or hydraulic installations and irrigation channels, in the Copiapó River this occurs when overflow of the channel occurs punctually along the river due to heavy rains or snowmelt episodes or the activation of the main tributary, Quebrada Paipote; a discharge perception threshold of 30 m^3/s is established for this category based on the documentary record; and (3) Catastrophic flooding or large flood, meaning the flood is generalized across the city causing severe damage or complete destruction of infrastructures not only adjacent but also close to the river including bridges, houses, railway tracks and roadways; in addition, there are large morphological changes to the river. In the Copiapó River this category is associated with overflow of the channel occurs along both the river and the main tributary, Quebrada Paipote. A discharge perception threshold of 180 m^3/s is established for this category based on the reconstructed discharges and the descriptions of the documentary record.

3.3. Flood deposits identification and dating

To complement the instrumental and historical archives, paleohydrology using flood deposits as indicators of flood stage (e.g., Benito et al., 2020a) was used. Stratigraphic and sedimentological analyses of the deposits were conducted. In the field, individual flood units were differentiated from other facies and identified using a variety of sedimentological indicators that included erosion surfaces or changes in sediment color, texture, and structures (Benito et al., 2003). Each flood deposit was sampled and sieved in the lab with a 2-mm sieve. The particle size distribution of the material passing the 2-mm sieve was measured using a Malvern Mastersizer 2000 at the facilities of the University of Huelva. The results were homogenized, expressed as a percentage of the distribution, and analyzed using the R package G2Sd (Fournier et al., 2014) which is an R (R Core Team, 2023) implementation of the GRADISTAT spreadsheet (Blott and Pye, 2001). Mean and sorting parameters of grain size were calculated using the logarithmic graphical method (Folk and Ward, 1957).

The sedimentary sequence chronology was determined using radiocarbon dating of peat layers collected along the section. Pre-treatment of the sample material for radiocarbon dating was carried out by Beta

Table 1
Radiocarbon dating samples and results for the geological section downstream Angostura canyon.

Sample ID	Lab code	Sample material	Age 14C (yr BP)	2σ calibrated age range
ANG-41	Beta - 503,282	Organic sediment	200 ± 30	1718–1814 CE
ANG-35	Beta - 510,255	Organic sediment	2180 ± 30	234–66 BCE
ANG-30	Beta - 503,281	Organic sediment	2400 ± 30	541–370 BCE

Table 2
Optically stimulated luminiscence dating results from flood deposits identified downstream Angostura canyon.

Sample ID	Depth (m)	Num. of aliquots	Dose rate (Gy/ka)	Equivalent Dose 2 ± 2σ (Gy)	OSL age ± 2σ (ka)	Calibrated year
ANG-48	0.3	2 (10)	2.28 ± 0.10	0.86 ± 0.08	0.377 ± 0.040	1602–1682 CE
ANG-47	0.3	0 (33)	2.48 ± 0.12	0.35 ± 0.03	0.141 ± 0.013	1865–1891 CE
ANG-46	0.7	2 (30)	2.47 ± 0.12	0.39 ± 0.02	0.159 ± 0.013	1847–1873 CE
ANG-45	0.9	1 (30)	2.39 ± 0.11	0.36 ± 0.02	0.152 ± 0.013	1854–1880 CE
ANG-44	1.15	0 (9)	2.54 ± 0.12	0.34 ± 0.06	0.133 ± 0.025	1861–1911 CE

Analytic Inc. (Miami, USA) as was the dating by AMS (accelerator mass spectrometry). Calibration of the radiocarbon dates was carried out using the Calib 7.0.4 (Stuiver et al., 2013) using the calibration curves SHCal13 for the Southern Hemisphere (Hogg et al., 2013). A summary of the samples submitted for dating is presented in Table 1. All ages are given in AD calendar years. Because of insufficient amounts of organic content in the Atacama Desert the flood deposit chronology was established employing OSL dating. Five OSL samples were collected by hammering stainless-steel tubes into the exposures. In addition, the surrounding sediment was collected for radionuclide analyses and undisturbed samples were taken to evaluate moisture content. The samples were analyzed at The Nordic Laboratory for Luminescence Dating of the Technical University of Denmark (Table 2).

3.4. Hydraulic modelling

Discharge estimates for the identified paleoevents were calculated by hydraulic modelling of the Angostura canyon (2200 m in length) using HEC-RAS (Hydrologic Engineering Center, 2010). This section of the river presents a mean slope of 0.0038 m/m and sinuosity index of 1.55. The HEC-RAS model was calibrated for the 2015 flood using discharge data estimations from the Dirección de Obras Hidráulicas (DOH, 2016). Cross sections were defined every 30 m and assigned Manning's n values of 0.07 and 0.035 for the valley floor and valley margins, were used according to Chow (2004). Palaeoflood discharges were estimated using the Standard Step Method (STM), the most commonly used method in palaeoflood hydrology (Webb and Jarrett, 2002).

3.5. Flood frequency analysis

Flood frequency analysis (FFA) was carried out on the maximum annual discharge series in Angostura for the period 1969–2020 and the

Table 3
Flood historical record Copiapó River 1650–2020. *S: summer season (Dec – May), W: winter season (Jun – Nov); ‡1: Minor flood; 2: Intermediate flood; 3: Large flood; †R: rainfall, S: snowmelting.

Year	Month	Season *	Flood category‡	Cause†	Documentary source
1655			3		Sayago, 1874
1746	Dec	S	1		Sayago, 1874
1787			2		Barreiro, 1929
1796	Jun	W	1	R	Sayago, 1874
1827	Jun	W	2	R	Sayago, 1874; Urrutia and Lanza, 1993
1833	Aug	W	1	R	Darwin, 1845 Newspaper El Amigo del País 14 and 18 Aug.1888 Meza et al., 1992
1835	?	?	1	R	Urrutia and Lanza, 1993
1844	Jul	W	1	R	Bowman, 1925 Newspaper El Atacameño 07.Jun.1927
1848	May	S	1	R	Urrutia and Lanza, 1993
1877	Jul	W	1	R	Mackenna, 1877 Urrutia and Lanza, 1993 Newspaper El Copiapino 02.Aug.1877
1888	Aug	W	3	R	Bowman, 1925 Urrutia and Lanza, 1993 Newspaper El Amigo del País 15/16/17/18/20. Aug.1888 Newspaper El Atacameño 15/16/17/18/20/21/23. Aug.1888 Newspaper El Mercurio de Valparaiso 18/20/22/25. Aug.1888 Municipal Act 08.Aug.1888 Letter from a neighbor to the Municipality Sep.1890
1890	Jun	W	1	R	Newspaper El Atacameño 16/17.Jun.1890
1893	Feb	S	1	R	Meza et al., 1992
1900	Aug	W	2	R	Newspaper El Atacameño 22.Aug.1900 Municipal Act 28.Aug.1900 Letter form the Major to the Home Office Minister 30. Aug.1900
1902	Jul	W	2	R	Urrutia and Lanza, 1993 Newspaper El Amigo del Pais 12/14/16.Jul.1902; Newspaper El Constitucional 11/12/14/15/16/17/18/20/23/25/26.Jul.1902 Municipal Act 11/12. Jul.1902 Letter form the Major to the Governor 13.Jul.1902 Congress law 1538, 24. Jul.1902
1905	May	S	1	R, S	Bowman, 1925
1905	Oct	W	1	R, S	Bowman, 1925
1906	Jan	S	2	S	Urrutia and Lanza, 1993 Newspaper El Mercurio de Valparaiso 10.Jan.1906 Newspaper El Amigo del Pais 7/9/10/13.Feb.1906 Zig-Zag Magazine 28. Jan.1906 Newspaper El Heraldo de Madrid 2.Mar.1906 Congress law 1795, 22. Jan.1906
1926	Feb	S	1	R	Newspaper El Atacameño 01/02/15/16/17/19/20/27.Feb.1926

(continued on next page)

Table 3 (*continued*)

Year	Month	Season *	Flood category‡	Cause†	Documentary source
1927	Jun	W	2	R	Newspaper El Atacameño 04/05/09/10.Jun.1927 Newspaper El Amigo del País 04/06/07.Jun.1927
1929	Jun	W	1	R	Newspaper El Atacameño 21.Jun.1929 Newspaper El Amigo del País 21/23/24.Jun.1929
1934	May	S	2	R	Newspaper El Atacameño 22/23/24/25.May.1934 Newspaper Los Angeles Times 22.May.1934 Newspaper New York Times 25.May.1934 Newspaper Chicago Daily Tribune 07.Jun.1934 Urrutia and Lanza, 1993
1938	Mar	W	2	R	Newspaper El Amigo del Pais 02/03/04/05. Mar.1938 Newspaper El Atacameño 02/03/04/05/07.Mar.1938 Newspaper The New York Times 05.Mar.1938 Urrutia and Lanza, 1993
1938	May	S	1	R	Newspaper El Amigo del Pais 23/24.May.1938 Newspaper El Atacameño 21.May.1938
1940	Jun	W	1	R	Newspaper El Amigo del País 13.Jun.1940 Newspaper El Atacameño 13.Jun.1940
1943	Jun	W	1	R	El Atacameño 29/30. Jun.1943 Meza et al., 1992
1962	Jul	W	1	R	Newspaper El Día 28/29. Jul.1962 Newspaper Fort Lauderdale News 28.Jul.1962
1980	Apr	S	1	R	Newspaper Atacama 07/08. Abr.1980 Meza et al., 1992
1987	Jul	W	2	R	Newspaper Atacama 28. Jul.1987
1988	Jan	S	1	S	Newspaper Atacama 11. Jan.1988
1991	Jun	W	1	R	Newspaper El Mercurio 18. Jun.1991
1997	Jun	W	2	R	Newspaper Atacama 13/14. Jun.1997 Newspaper El Mercurio 13/14.Jun.1997
1997	Aug	W	1	R	Newspaper Atacama 18/19/20.Aug.1997
2011	Jul	W	1	R	TVN news
2015	Mar	S	3	R	Newspaper El Diario de Atacama 26/27.Mar.2015 You Tube videos Izquierdo et al., 2021
2017	May	S	2	R	Newspaper El Diario de Atacama 14/15.May.2017

non-systematic record based on palaeoflood discharge estimates. The frequency analysis was performed using the AFINS 2.0 software (Botero and Francés, 2006). The most robust results in terms of adjustment to the drawn plotting positions were obtained with a log Gumbel distribution and a Two Component Extreme Value (TCEV) distribution. The parameters set for these statistical functions have been estimated by the Maximum Likelihood Estimation (MLE) method (Stedinger and Cohn, 1986).

3.6. Hydroclimatic variability and climatic oscillations

The Standardized Precipitation Index (SPI) (McKee et al., 1993) quantifies the precipitation deficit for different time scales and represents the number of standard deviations of precipitation in each accumulation period (12 months) with respect to the mean, after converting the original distribution to a normal distribution. The analyzed periods were classified as: Extremely Dry $\leq$2; Severely Dry -1.5 to -1.99; Dry -1.49 to -1; Normal -0.99 to 0.99; Wet 1 to 1. 49; very Wet 1.5 to 1.99; and Extremely Wet $\geq$2. In addition, the periods were characterized considering their duration (length of the period), intensity (maximum value in a period) and magnitude (sum of the SPI values of a period). The frequency of occurrence of wet and dry cycles was estimated for SPI-12 (Ayugi et al., 2020) dividing the times series in four periods: 1888–1900; 1901–1950; 1951–2000; 2001–2020.

To assess potential drivers of the hydroclimatic variability recorded in the SPI, we analyzed its relationship with three sea surface temperature indices obtained from the NOAA – Climate Prediction Center (CPC): the Niño 3.4 index for the series 1854–2020, the Pacific Decadal Oscillation (PDO) index for the series 1900–2020, and the Atlantic Multidecadal Oscillation (AMO) index for the series 1850–2020. The correlation was carried out by conducting a moving average of the indices in accumulated periods of 1 to 20 years. Finally, gauge and reconstructed records were compared with the indices most linked to the rainfall variability to evaluate the role of these climatic indices in the Copiapó river floods.

4. Results

4.1. Historical flood events in the Copiapó River

After an exhaustive review of original sources (newspapers, etc.) 36 flood events have been identified since 1650 (Table 3). This list includes all events that have occurred in the middle and lower parts of the Copiapó river and does not consider the upper part of the basin, upstream of the Lautaro dam, where some extraordinary events have occurred such as the recent 1985 glacial lake outburst flood (Iribarren Anacona et al., 2018).

4.1.1. Documentary period (1650–1970)

The documentary period (1650–1970) encompasses twenty-seven events from which only one occurs before the official establishment of the city in 1744; the 1655 flood. The event is surprisingly well described two hundred years after its occurrence by Sayago (1874) evidencing its magnitude. At the time, Copiapó was a small village with scattered houses although at least 4000 people were settled along the valley (Orellana, 2005). The flow severely modified the valley and important geomorphological changes are described including erosion of large volumes of sediment in wetlands used for grazing, damage to crops and the destruction of a church upstream from the present location of the city.

Three events are mentioned during the 18th century, after the founding of the city. Two of them only caused minor damage in irrigation channels (1746 and 1796 floods; Sayago, 1874) while for the third one (1787 flood) evacuation was needed as the flow reached the streets and some houses were damaged (Barreiro, 1929). More prolific descriptions exist for the 10 flood events that occurred during the 19th century as journalism developed in this period and a rain gauge was installed in 1863 in Copiapó making easier identifying large or heavy rainfalls that may led to floods. The 1833, 1835, 1844, 1848, 1877, 1890 and 1893 events were minor floods in which the inhabitants describe the rise of the flow in the river or its main tributary with joy when it happens after a dry period, but generally with the fear of a potential flood although in all the cases mostly irrigation ditches were damaged (Sayago, 1874; Darwin, 1845; Meza et al., 1992; Bowman, 1925; Urrutia and Lanza, 1993). During the winter months of 1827 and 1900

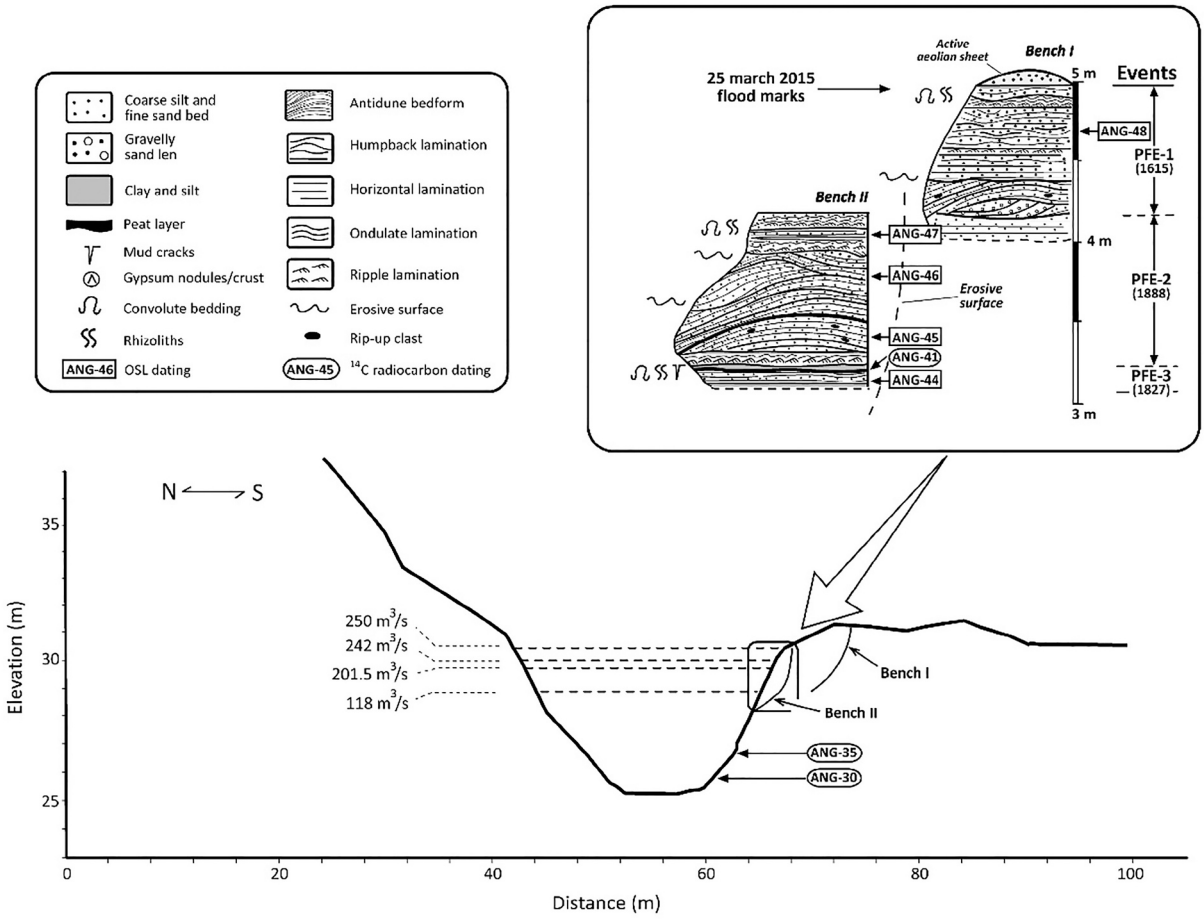

Fig. 2. Stratigraphic section of Angostura site and its position in the valley cross-section. The location of the dated samples by radiocarbon and OSL is indicated as well as the calculated discharge estimates associated with flood deposits and the 2015 event.

extraordinary floods occurred. These events caused an overflow of the river or its tributary causing in both cases damage to farms and houses. In particular, on August 22, 1900, the riverbanks were overflowed after the July and August rains caused some neighbors to take refuge in the San Francisco convent and days later the mayor sent a letter to the Home Office Minister in Santiago asking for financial support for the victims (City Archive).

The largest flood event of the 19th century took place on August 14, 1888. On August 13 and 14, the rain gauge of Copiapó recorded a total of 36.8 mm (Bowman, 1925). As a result of these rains, probably greater in the Andes, the flow of the Copiapó River increased and overflowed the middle valley upstream the city and Quebrada Paipote activated and flooded the town of San Fernando (now part of the city of Copiapó) located in the junction with the Copiapó river causing several fatalities. El Atacameño newspaper makes in its edition of August 18 a detailed description of the damage that allows us to reconstruct the flood extension in the city in approximately 2 km^2 and the flood depth at some points including a reference of a 1.5 m water depth at the historic building of the current campus of the University of Atacama. The newspaper describes that the flood caused 11 deaths in Copiapó and Tierra Amarilla (upstream the main city) and hundreds of houses resulted with non-repairable or major damage. During the 20th century documentary period, before a discharge gauge was in operation for the river, 13 flooding events occurred. The May 1905, October 1905, 1926, 1929, May 1938, 1940, 1943 and 1962 were minor flood events in which the flow damaged or destroyed bridges and the roads and railroads adjacent to the channel. *El Amigo del País* newspaper stated in a June 13, 1940 article that the water flow in the Paipote channel was 10 m wide and 0.7 m deep. These data results in a minimum discharge of 13.7 m^3/s for this event calculated using a Manning n value of 0.017. The Paipote channel construction started after the March 1938 extraordinary flooding event in which >40 cm of water flooded houses, damaged the railroad station, and swept away hundreds of meters of railroad tracks. The economic damage was estimated at 300,000 Chilean pesos and the international impact was so important, due to the decrease in the mineral exports, that even The New York Times newspaper published a short telegram informing about the event entitled “Storms and floods sweep North Chile”. Other intermediate events were those occurring in 1902, 1906, 1927 and 1934. The January 1906 flood occurred after the rains and snows of the 1905 winter, the snowmelt caused a large increase in the flow that, according to the ZigZag magazine, reached 4 m/s and eroded the valley floor leaving the check gates of the irrigation ditches above the new riverbed.

4.1.2. *Instrumental period (1970–2020)*

The instrumental gauging data series in Copiapó begins in 1970 and since then, nine flooding events have occurred. The 1980, 1988, 1991, August 1997 and 2011 were small floods that did not exceed the 30 m^3/s threshold and only caused damage in or near the channel. By contrast, the 1987, June 1997 and 2017 intermediate floods did exceed that threshold and caused much more damage in the city. During the June 1997 event the highest rainfall intensity of the instrumental time series was recorded (68.3 mm in 14 h) as the storm was centered above the city instead of upstream. >20,000 people were affected and seven people died. Finally, the March 2015 flood event catastrophically affected 72% of the urban area of Copiapó when a mudflow buried the streets with a

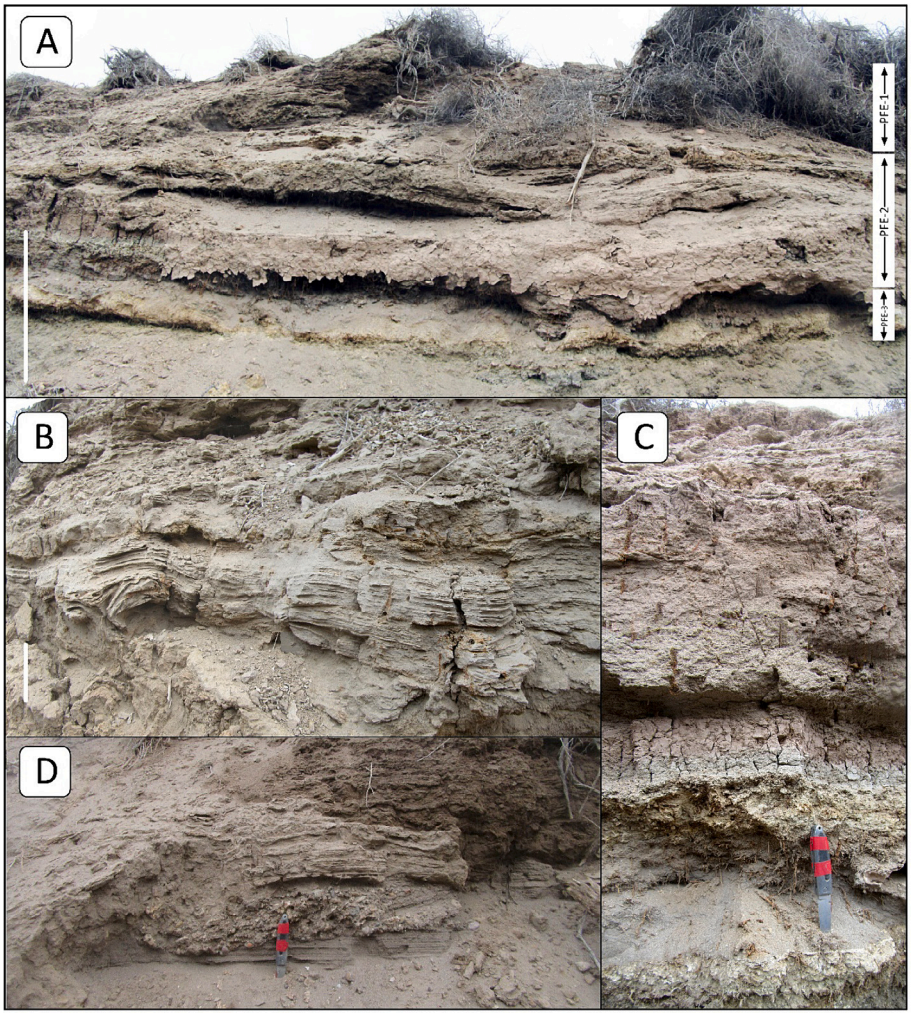

Fig. 3. Photographs of paleoflood deposits at the Angostura site. A) Amalgamated lenticular sets showing a distinctive wavy bedform geometry characterized by stacked low-relief antiforms and trough crossbedding (humpback cross-lamination) in PFE-2 (scale bar 100 cm). B) In phase climbing ripples, laminae, and gently undulated lamination at the top of PFE-2 with water escape structures (scale bar 15 cm). C) Clay layer with mud cracks intercalated between PFE-3 (below) and PFE-2 (above). D) Upstream-dipping trough backset filling troughs formed by cross-bedded sand and gravel deposits at the base of PFE-1. Knife (15 cm). Flow from left to right in all the cases.

sandy mud deposit of >30 cm in thickness that caused major or non-repairable damage to >1300 houses across the city (Izquierdo et al., 2021). The flood was caused by a cutoff low with anomalous heights that moved east and coincided with extraordinary high precipitable water (Barrett et al., 2016; Bozkurt et al., 2016; Valdés-Pineda et al., 2018). The associated rainfall varied between 10 mm from the coast and > 85 mm in the high mountainous area. Although none of the gauging stations recorded the peak discharge of the flood the DOH (2016) reconstructed the maximum flow at the city and at Angostura of 220 m^3/s and 242 m^3/s, respectively.

4.2. Flood deposits and paleodischarge estimation

The section located in Angostura site consists of a flood bench 4.6 m in thickness on the left margin of the Copiapó River, 150 m downstream of the canyon exit (Figs. 1 and 2). The sedimentological analysis reflects a complex stratigraphic architecture, with the overlapping of two benches that is only observable in the upper part of the river margin and that was clearly revealed by the OSL dating (Fig. 2). The section is formed by silt, sand and peat deposits, with common formation of paleosoils in its middle and lower part that date from 541 to 370 BCE to 234–66 BCE. These deposits indicate the formation of a fluvial wetland and other fluvial channel deposits not analyzed in this work.

In the upper part of the section, very well sorted coarse silt and fine sand beds of decimetric thickness occur with fine-grained deposits of charcoal and silt interbedded. Here, three paleoflood deposits have been identified with very similar sedimentologic characteristics (Paleoflood Event, PFE-1 to 3 in Fig. 2). The highest flood deposit (PFE-1) is associated with a minimum discharge estimate of 250 m^3/s, while a minimum discharge estimate of 201 m^3/s is required for a flood event to cover PEF-2 and 118 m^3/s to cover the PFE-3 deposits. In addition, the 2015 flood (242 m^3/s) covered the higher part of the outcrop with a thin mud line and the accumulation of dead plants that stands as a stage indicator of the water level of this last event. These marks were used by DOH (2016) to reconstruct the peak flow near the stream gauging station. The paleoflood deposits are separated by erosion surfaces and their thickness range between 10 and 95 cm. All of them includes horizontal and sigmoidal to low-angle lamination, sometimes with minor-concave and convex-upward forms (humpback cross-lamination) (Fig. 3A), as well as in phase climbing ripples laminae and gently undulated lamination (Fig. 3B). Soft-sediment deformations, such as convolute lamination are very common in the sandy sediments. Some plant debris and rip-up clasts are incorporated in the lower part of the sedimentary sequence, while silty clay and charcoal deposits with mud cracks and gypsum nodules occasionally occur at the top of the flood beds (Fig. 3C). These indicators of subaerial exposure were used to determine the end of

the flood event and discriminate the three individual flood units. Quartz OSL dating of these deposits has revealed a complex three-dimensional architecture of two overlapping benches (Fig. 2). PFE-1 was dated to 377 ± 40 years while PFE-2 and PFE-3 resulted in an average date of 146 ± 13 years.

The lower to middle part of PFE-1 and PFE-2 show a distinctive wavy bedform geometry characterized by stacked low-relief antiform (convex upward) and trough cross-bedding with sharp erosive base. The wavelength of the bedforms is 90–135 cm, and their amplitude ranged 10–25 cm in PFE-2, where 3 amalgamated lenticular sets occur with a total thickness of 95–135 cm. A well-defined upstream and downstream lamination is the dominant internal structure within these deposits. The laminae are concordant with the lower bounding surfaces in most of the cases and may be locally separated by mud drapes or very thin charcoal layers. The top of the antiforms is often truncated by minor erosion surfaces, while some upstream-dipping backset is preserved filling the troughs formed by cross bedded sands and gravels deposits (Fig. 3D). These characteristic bedforms can be observed along >50 m at the top of the bench in both river margins of the main fluvial channel (Fig. 2).

5. Discussion

5.1. The last 400 years flood events in the southern Atacama Desert

Twenty-two of the thirty-six flood events that have been identified over the last 400 years have been classified as small floods or ordinary rises in river flow. These occur in the Copiapó River after heavy rains or snowmelt episodes, when a slight increase in flow happens and minor damage to irrigation infrastructure may occur. Among these, two events occurred in the 18th century, seven during the 19th century, twelve in the 20th and 21st centuries (Table 3). As these events do not exceed a perception threshold, they are not normally retained in the society memory and thus, it is easier to identify those that are more modern.

The historical record includes eleven intermediate floods in which the flooding was confined to areas adjacent to the river causing damages in irrigation channels or infrastructures located near the channel such as railway tracks, roads, or farms. Only three have occurred during the instrumental period (1987, June 1997 and 2017 floods) although there is only measured data for the 1987 event as the 1997 exceeded the gauging station and in 2017 the station was still damaged by the 2015 flood event. The other eight extraordinary flooding events occurred in the 18th century (one event), the 19th century (two events) and the historical period of the 20th century (five events), all exceeding the discharge perception threshold of 30 m^3/s established for this category. This is the case of the PFE-3 whose deposit was described in the Angostura section with a minimum discharge value of 118 m^3/s. This discharge value together with the radiocarbon and OSL dating associates this deposit with the 1827 flood.

Finally, a total of 3 catastrophic flooding events, with discharge values >180 m^3/s, have been identified in the last 400 years, 1655, 1888 and 2015 floods. The OSL ages obtained for the topmost flood deposits in the Angostura section establish that PFE-2 occurred in the 19th century while PFE-1 took place in the 17th century. The large magnitude of PFE-1 and 2 with discharges >200 m^3/s suggest that they likely correspond to the largest historical floods i.e. 1655 and 1888 respectively. The August 13 and 14, 1888 flood is the first in which an exhaustive inventory of the damages is carried out and in the descriptions of the newspapers they provide flood depth measures at some points in the streets of the city of Copiapó that were similar or even higher to those of 2015. This flood event remains as the reference flood until the mid-20th century as in every news of category 2 or 1 floods, or even only heavy rainfalls, the 1888 flood is mentioned by the journalists. The 1655 flood is only mentioned by Sayago (1874) but its deposit indicating a minimum discharge value of 250 m^3/s, slightly larger than the 2015 flood, confirms the category of this flood. In fact, the descriptions of Sayago (1874) were written 200 years after the event, but the flood appears mentioned up to 5 times and not only because it destroyed a church. The author describes (p. 320–321) how the river increased its flow and eroded the valley causing large gullies in the wetlands that remained until the chronicle's date. Similar extreme erosion occurred during 2015 at different points of the valley where the riverine wetlands were completely washed away by the flow that caused strong lateral erosion and entrenching of the river channel (up to 10 m deep) (Sparelli et al., 2018). These major geomorphological changes had impacts in the 1655 valley economy as they caused legal conflicts for the lost lands and for those that were positively affected by the flood (Sayago, 1874).

The similar impacts of the 1655 and 1888 destructive floods in the Copiapó Valley described in the historical chronicles with the dated flood deposits of Angostura site is supported not only by the paleodischarge reconstruction, but also by the sedimentary features of the high-energy facies. The paleoflood deposits of Angostura section present clear similarities with the high-stage flood facies defined by Benito et al. (2003) formed in a channel widening environment during the first stages of the event when the flow extends into lateral marginal areas covering the bench. The parallel horizontal lamination and ripple laminae observed record the alternating flow conditions result in current ripple migration to upper plane bed migration when velocities increase. The conspicuous occurrence of climbing ripples and undulate parallel lamination are interpreted as the vertical aggradation of sediments produced by an increasing in the fallout from suspension combined with the ripple migration when the water current decelerates during the flooding (e.g., Ashley et al., 1982; Baas et al., 2021). Occasionally, the rapid and intermittent decrease in the flow velocity generated mud drapes and the settling of organic-rich very thin laminae into the high-energy deposits. On the other hand, the horizontal/sigmoidal lamination to low angle cross-lamination very probably indicate the progressive increasing flow power at transitional conditions from the dune stability field into the upper plane bed field under massive rates of sediment fallout (Chakraborty and Bose, 1992; Fielding, 2006). Finally, the remarkable occurrence of fluid escape structures can be explained by density inversion in sediment layers with grain sizes very susceptible for the synsedimentary deformational structures formation as the convoluted bedding (Lowe, 1975; Benito et al., 2003).

The wavy beds of PFE-1 and PFE-2 are very similar to antidunes in the sense of Araya and Masuda (2001) and Fielding (2006). The antidunes record the formation of stationary (stable) waves and upstream migrating bedforms (unstable) in the channel belt (Cartigny et al., 2014). The formation of these structures occurs at higher flow velocities than upper plane bed, when low relief bedforms formed at the transition from subcritical flow to supercritical flow (waves in-phase with the bedforms) or directly under supercritical flow (unstable conditions and wave break upstream). Their formation is commonly associated with shallow water and very fast sedimentary aggradation (Lang et al., 2020).

During the waning flood stage, the flow velocity is low and generate the sedimentation of plant debris and fine-grained sediments, producing low-energy flood deposits. Thus, the end phase of the event is characterized by the formation of thin layers of fine-grained sediments and charcoal on the top of the high-energy flood deposits. The subaerial exposure conditions resulting in the formation of mud cracks and gypsum nodules/crust on the top of the paleoflood deposits some weeks or months after the event.

The spectrum of sedimentary structures recognized at the Angostura site represent the successive floods of a zone located near the main fluvial channel by moderate to very high-energy flows accompanied by high suspended sediment concentration during the paroxysm of the events. The intermittent transition conditions from lower to high flow regimen and the subsequent waning phase of the flood event are recorded in the sedimentary sequences. This facies resembles some architectural elements of the "Laminated Sand Sheets" architectural element of Miall (1985) and the most recent "Upper Flow Regime Sheets, Lenses and Scour Fills" elements of Fielding (2006). Both are associated to transitional to upper flow regime conditions with high rate

Table 4
Flood quantiles for different return periods in Angostura for a log Gumbel and a two-component extreme value (TCEV) distribution fitted to, firstly the annual maximum systematic records only and secondly, to the combined systematic and non-systematic discharges.

Exceedence annual probability (%)	Average recurrence interval (years)	Peak discharge (m^3/s)			
		Log Gumbel		TECV	
		Systematic record	Sys + paleofloods	Systematic record	Sys + paleofloods
20	5	1.2	3.8	0.7	39.4
10	10	2.2	9.9	23.3	72.1
4	25	4.6	32.7	55.5	113.3
2	50	8.1	79.4	79.4	144.0
1	100	14	191.5	103.0	174.1
0.2	500	50.1	1464	157.0	243.3
0.1	1000	86.6	3510	179.7	271.7

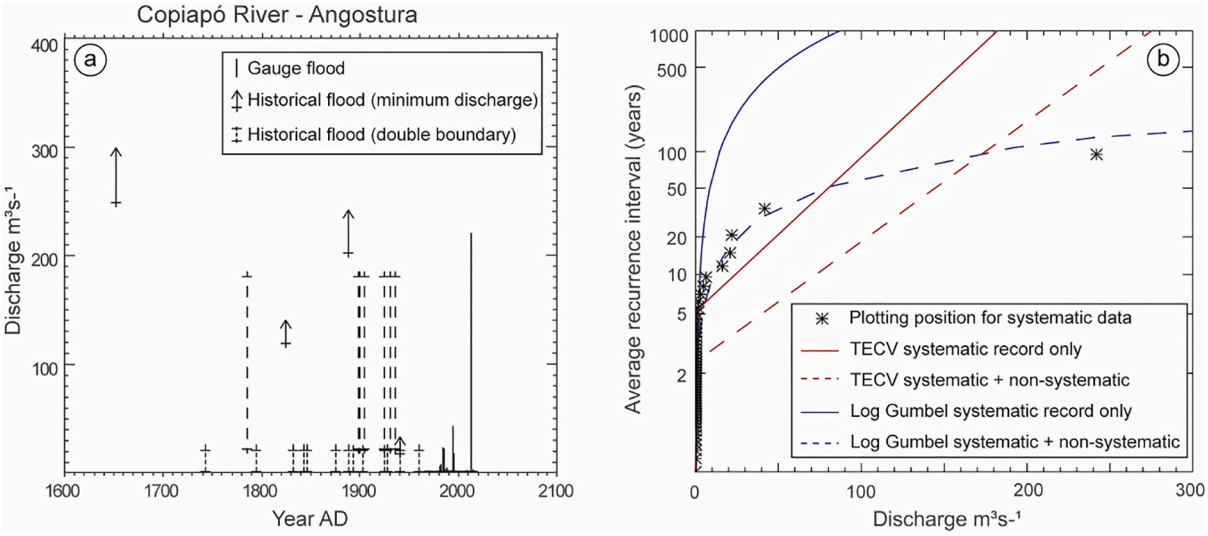

Fig. 4. a) Temporal distribution of the flood discharges data as it was entered for the flood frequency analysis. The bottom of arrows indicates the estimated minimum discharge for historical floods reconstructed from the flood deposits position. Vertical dashed lines indicate the double boundary of the historical floods according to the assigned category. The vertical bars (post-1969) are the maximum annual discharge values (systematic data) at the Angostura gauging station; b) Two Component Extreme Value (TCEV) and Log-Gumbel distributions fitted with systematic data only and systematic + non-systematic data.

of sandy sediment accumulation under the influence of a strongly seasonal peak in runoff during hydrological conditions characterized by abrupt floods and drops in the flow stages.

5.2. Flood frequency analysis

The flood frequency distribution providing the best performance in the combination of non-systematic (censured) and systematic data was the log Gumbel distribution function. Discharge values associated with different annual exceedance probabilities (recurrence intervals) are shown in Table 4. The incorporation of the non-systematic data (historical and paleohydrological) into the FFA results in an increase of the magnitude of the flood quantiles when compared with the ones obtained with the systematic record (Fig. 4). For instance, the catastrophic flood perception threshold represents a 1.1% annual probability flood in the combined systematic and non-systematic data (i.e., an average recurrence interval of 120 years) while it is a 0.04% in the systematic data analysis.

5.3. Multi-decadal flood patterns and climate variability

As most of the flood events were caused by rain episodes (29 out of 36) we analyze the role of rainfall distribution in the temporal flood pattern. The compiled time series includes annual precipitation in Copiapó from 1795 to the present (228 years) and it shows a mean annual value of 22.5 mm with a maximum rainfall recorded of 149.7 mm in 1997 (Fig. 5). Years with no rain represent 18% of the series. In addition, 34% of the series corresponds to years in which rainfall is <6 mm and 53% to years in which the precipitation is <20 mm. Rainfall shows a decreasing trend. The longest period without precipitation corresponds to the period 1993–96, four years in a row in which it did not rain. In the time series there is a clear cyclicality that Valdés-Pineda et al. (2018) attribute to the cyclicality of the PDO until the middle of the 20th century.

The Standardized Precipitation Index (SPI) of Copiapó weather station was obtained using the monthly precipitation series 1888–2020 for a 12-month accumulation period (Fig. 5). Wet and dry years depend on the value taken by the index: values greater than +1 are considered wet, while values below than −1 are considered dry (McKee et al., 1993). Consequently, wet periods are the sum of consecutive wet years, while dry periods are the sum of consecutive dry years. In the time series, 20 wet periods and 26 dry periods can be identified (Fig. 4). The longest wet period occurs from 1926 to 1931, with a magnitude of 93.71 and an intensity of 2.07, whereas the longest dry period occurs from 1993 to 1997. From 1888 to 1953 wet cycles of greater magnitude and longer duration are observed while at the middle of the last century a slight trend towards shorter (lower magnitude) and less intense wet cycles appears (Table 5).

Traditionally, extraordinary rains in the Atacama Desert have been related with positives phases of the ENSO (e.g., Ortlieb, 1995). In fact, according to Houston (2006b) during El Niño years, winter rainfall tends to be higher than average, while higher rainfall in the summer months is

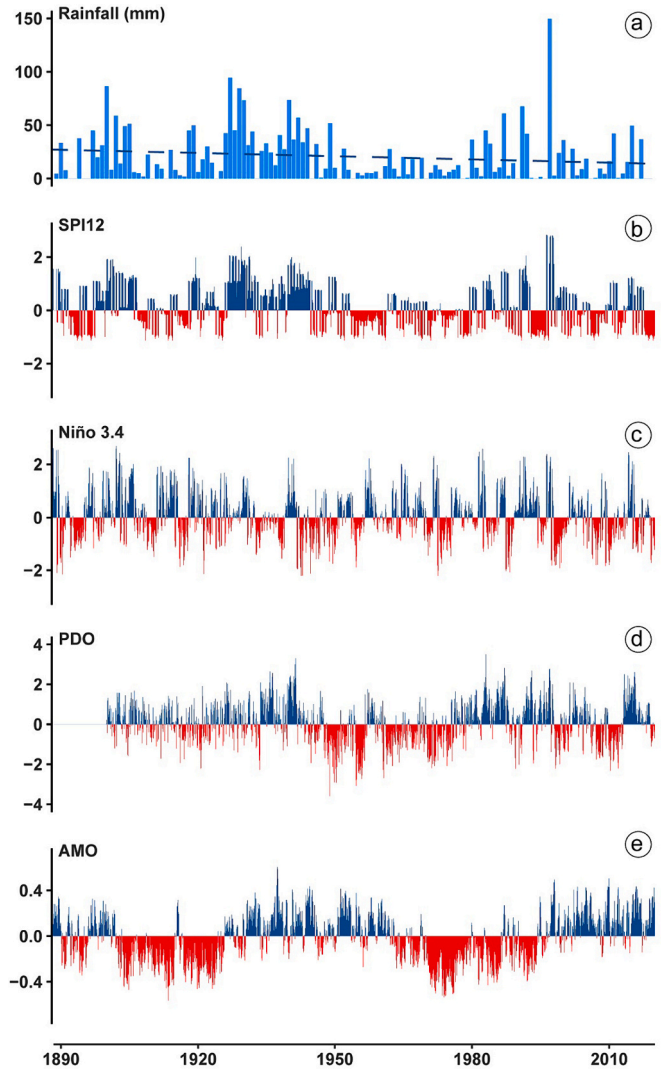

Fig. 5. a) Annual precipitation in Copiapó for the time series 1888–2020; b) SPI values for Copiapó calculated for the 1888–2020 series of periods of 12 months (SPI-12) with negative values in red and positive values in blue; c) Niño 3.4 index for the time series 1888–2020 showing positive anomalies in blue (El Niño conditions) and negative anomalies in red (La Niña conditions); PDO index for the time series 1900–2020 showing positive anomalies in blue and negative anomalies in red; e) AMO index for the time series 1888–2020 showing positive anomalies in blue and negative anomalies in red. (For interpretation of the references to color in this figure legend, the reader is referred to the web version of this article.)

related to La Niña phenomenon. However, Valdés-Pineda et al. (2018) have recently explored patterns of precipitation fluctuating over a period longer than 30 years in Chile. These authors found a significant multi-decadal precipitation cycle between 40 and 60 years in its subtropical and extratropical regions, i.e., at the study area latitude, that seems to be largely linked to PDO and AMO modulation. At Copiapó, the Niño 3.4 index (Fig. 6 left) shows positive correlations with SPI-12 in the months of March, April, and May, being May the month with the most positive correlation (+0.5). The rest of the months show a positive correlation at time scales from 1 to 10 years, while the winter and spring months show a negative correlation with SPI-12 at time scales from 13 to 20 years. On the other hand, the PDO (Fig. 6 center) shows positive correlations in all months and in all scales with the SPI-12 index, especially in the months of July (+0.9) and December, at time scales from 10 to 20 years. Finally, the AMO (Fig. 6 right) shows a positive correlation with the reconstruction, especially from May to July, with the highest correlation obtained in June (+0.36) when averaged over 19 years.

Rainfall at Copiapó is clearly largely modulated by the PDO and it is then, natural to expect an impact of the PDO on flooding in the Copiapó river. Fig. 7 shows the relationship between the monthly PDO index, and the maximum discharges recorded during those months from the Angostura gauging station and the reconstructed paleodischarges. The majority of historical floods since 1900 have happened during the positive phase of the climatic index, with only two category one events (1991 and 2011) occurring outside of this period, making the connection between this index and floods in the Copiapó River clear. In fact, discharges >30 m^3/s, i.e., intermediate and large floods, occur with positive phases of the PDO.

Superimposed to the PDO, the ENSO phase has clearly an effect on the floods as only the 2011 occurred with a negative anomaly of the sea surface temperature (Fig. 7). Recently, Freund et al. (2019) suggest that stronger rainfall events modulated by ENSO and ENSO-like conditions will impact this arid to semiarid region in a future climate scenario, similar to those developing in the Pacific during 2023 in which the total number of associated floods may decrease while high-magnitude floods may increase (Ortega et al., 2019) having a large impact on local communities. As changes in flood frequency over multi-millennial and multicentennial scales have been linked to climatic regimes and changes in atmospheric circulation modes (Wilhelm et al., 2019), the identification of such connections through future palehydrological studies of the Copiapó River dynamic during the last millenia will provide a basis for potential improvements of hydrological projections in the context of the ongoing climate change as flood magnitude and frequency are expected to change.

6. Conclusions

After the catastrophic March 2015 flood event a better understanding of the Copiapó River flood history was needed in order to accurately assess how extraordinary that event was and how its fluvial dynamic

Table 5
Wet and dry periods frequency for the SPI-12 index in Copiapó and flood events in the Copiapó river. Extremely wet years show their SPI-12 index value in parenthesis. *Extremely wet year with a flood event.

	Number of wet months	Number of dry months	Extremely wet years	Minor flood	Intermediate flood	Large flood
1888–1900 (156 months)	29 (18.6%)	9 (5.8%)		2	1	1
1901–1950 (600 months)	190 (31.7%)	14 (2.3%)	1927 (+2.07)* 1928 (+2.05) 1929 (+2.40)* 1931 (+2.05) 1940 (+2.01)*	7	5	0
1951–2000 (600 months)	58 (9.7%)	24 (4.0%)	1992 (+2.06) 1997 (+2.84)* 1998 (+2.82)	5	2	0
2001–2020 (240 months)	20 (8.3%)	10 (4.2%)		1	1	1

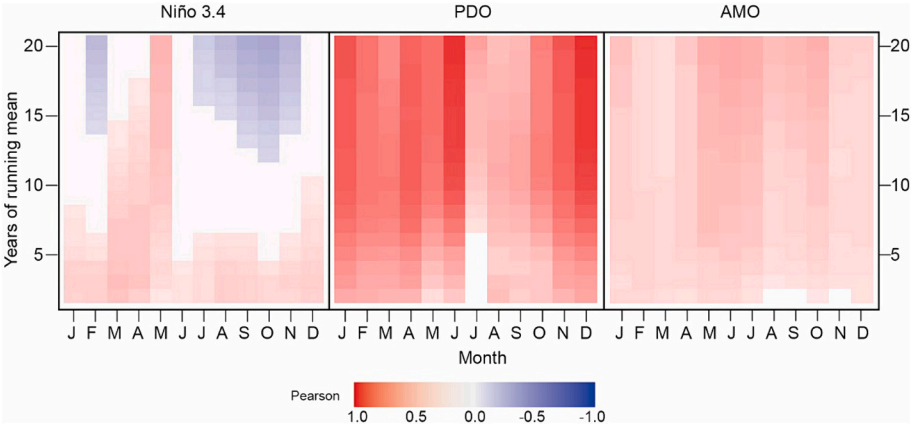

Fig. 6. Correlation between the three indices of climate variability (left: Niño 3.4 index; center: PDO, Pacific Decadal Oscillation index; and right AMO, Atlantic Multidecadal Oscillation Index) and the reconstructed SPI-12. The correlations were computed by months (X axis) and moving average windows (Y axis). Only Pearson correlation values at the >0.01 significance level are shown.

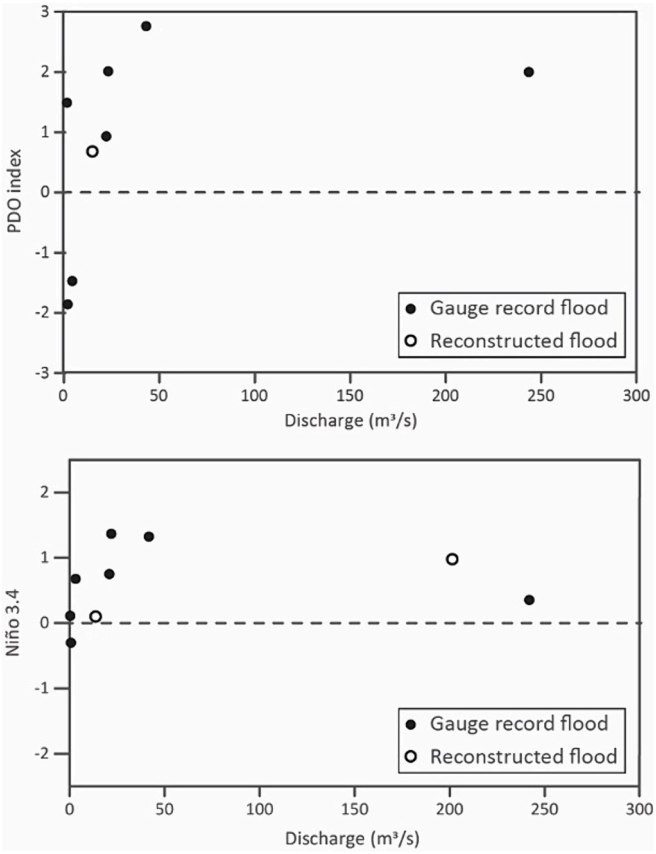

Fig. 7. Above: Relationship between monthly PDO index values and measured and reconstructed discharge of historical floods in the Copiapó River at Angostura since 1900; Below: Relationship between monthly Niño 3.4 index values and measured and reconstructed discharge of historical floods in the Copiapó River at Angostura since 1888.

relates with global climate oscillations. They study of the instrumental and documentary record of the floods occurred during the Chilean historical period in this arid basin of the southern Atacama Desert has allow identifying 36 events in the last 400 years that were categorized after their historical descriptions. In addition, three flood deposits corresponding to the historical period have complemented the historical information allowing their paleodischarge reconstruction. Twenty-two events were classified as ordinary rises of the river flow (discharges <30 m^3/s), eleven as intermediate floods in which the damage is confined to areas adjacent to the river (discharges 30–180 m^3/s), and only three as catastrophic floods (discharges >180 m^3/s) (1655, 1888 and 2015 floods). The incorporation of the historical and paleohydrological data into the flood frequency analysis results in an increase of the magnitude of the flood quantiles in which large flood events occur with an average recurrence interval of 120 years. Most of the flood events were caused by heavy rains that are largely linked to the PDO and the AMO with a superimposed effect of the ENSO. In fact, discharges >30 m^3/s, i.e., intermediate and large floods occur with positive phases of the PDO and the ENSO. Further exploration of the fluvial geological record of the Copiapó River will help lengthening to thousands of years the flood record and understanding its connection with the climate variability in the past. This response can then be projected to the expected climate scenario with stronger rainfall events modulated by ENSO and ENSO-like conditions that may lead to a decrease in the total number of associated floods but to an increase in the high-magnitude floods. Anticipating these changes will help understanding disaster risk in this arid region and improving communities' resilience.

CRediT authorship contribution statement

Tatiana Izquierdo: Conceptualization, Data curation, Formal analysis, Funding acquisition, Methodology, Writing – original draft, Writing – review & editing, Project administration, Supervision. **Ai-ling Rivera:** Data curation, Investigation, Writing – review & editing. **Ángela Galeano:** Investigation, Methodology, Software, Writing – review & editing. **Diego Gallardo:** Software, Writing – review & editing. **Verónica Salas:** Software, Writing – review & editing. **Olga Aparicio:** Software, Writing – review & editing. **Jan-Pieter Buylaert:** Resources, Writing – review & editing. **Francisco Ruiz:** Investigation, Resources, Writing – original draft, Writing – review & editing. **Manuel Abad:** Conceptualization, Data curation, Investigation, Supervision, Writing – original draft, Writing – review & editing.

Declaration of competing interest

The authors declare the following financial interests/personal relationships which may be considered as potential competing interests:

Tatiana Izquierdo reports financial support and article publishing charges were provided by Rey Juan Carlos University.

Data availability

Data will be made available on request.

Acknowledgements

The authors acknowledge ANID (Agencia Nacional de Investigación) for its financial support through grant FONDECYT (Fondo Nacional de Desarrollo Científico y Tecnológico) 11160405 (COPIFLOOD project) and Universidad Rey Juan Carlos for its financial support through the IMPULSO project VARHIDRO (M2994). The authors also thank Mabel Tapia for her assistance at the Municipal Archive of Copiapó, Guillermo Cortés and Rodrigo Zalaquett for their support at the Atacama Regional Museum Archive, and Eduardo Fritis for his help in the transcription of the historical documents. In addition, we thank the anonymous reviewers and the editor, Ian Fuller, for their careful reading of our manuscript and their many insightful comments and suggestions.

References

Abraham, E.M., Rodríguez, M.D., Rubio, M.C., Guida-Johnson, B., Gómez, L., Rubio, C., 2020. Disentangling the concept of "South American Arid Diagonal". J. Arid Environ. 175, 104089 https://doi.org/10.1016/j.jaridenv.2019.104089.

Almeyda, E., 1948. Pluviometría de las zonas del desierto y las estepas cálidas de Chile.

Araya, T., Masuda, F., 2001. Sedimentary structures of antidunes. An overview. J. Sedimentol. Soc. Jpn. 53 (53), 1–15. https://doi.org/10.4096/jssj1995.53.1.

Ashley, G.M., Southard, J.B., Boothroyd, J.C., 1982. Deposition of climbing-ripple beds: a flume simulation. Sedimentology 29, 67–79.

Ayugi, B., Tan, G., Niu, R., Dong, Z., Ojara, M., Mumo, L., Babaousmail, H., Ongoma, V., 2020. Evaluation of meteorological drought and flood scenarios over Kenya, East Africa. Atmosphere 11 (3), 307. https://doi.org/10.3390/atmos11030307.

Baas, J.H., Best, J., Peakall, J., 2021. Rapid gravity flow transformation revealed in a single climbing ripple. Geology 49. https://doi.org/10.1130/G48181.1.

Baker, V.R., 2000. South American paleohydrology: future prospects and global perspective. Quat. Int. 72, 3–5. https://doi.org/10.1016/S1040-6182(00)00016-1.

Baker, V.R., Benito, G., Brown, A.G., Carling, P.A., Enzel, Y., Greenbaum, N., Herget, J., Kale, V.S., Latrubesse, E.M., Macklin, N.G., Nanson, G.C., Oguchi, T., Thorndycraft, V.R., Ben Dor, Y., Zituni, R., 2022. Fluvial palaeohydrology in the 21st century and beyond. Earth Surf. Process. Landf. 47, 58–81. https://doi.org/10.1002/esp.5275.

Barreiro, A.J., 1929. El viaje científico de Conrado y Cristián Heuland a Chile y Perú: organizado por el gobierno español en 1795. Publicaciones de la Real Sociedad Geográfica, Madrid, 127 pp.

Barrett, B.S., Campos, D.A., Veloso, J.V., Rondanelli, R., 2016. Extreme temperature and precipitation events in March 2015 in central and northern Chile. J. Geophys. Res.-Atmos. 121 https://doi.org/10.1002/2016JD024835.

Barriendos, M., Coeur, D., Lang, M., Llasat, M.C., Naulet, R., Lemaitre, F., Barrera, A., 2003. Stationarity analysis of historical flood series in France and Spain (14th–20th centuries). Nat. Hazards Earth Syst. Sci. 3 (6), 583–592. https://doi.org/10.5194/nhess-3-583-2003.

Benito, G., Sánchez-Moya, Y., Sopeña, A., 2003. Sedimentology of high-stage flood deposits of the Tagus River, Central Spain. Sediment. Geol. 157, 107–132. https://doi.org/10.1016/S0037-0738(02)00196-3.

Benito, G., Lang, M., Barriendos, M., Llasat, M.C., Francés, F., Ouarda, T., Thorndycraft, V.R., Enzel, Y., Bardossy, A., Coeur, D., Bobée, B., 2004. Use of systematic, palaeoflood and historical data for the improvement of flood risk estimation, Review of scientific methods. Nat. Hazards 31 (3), 623. https://doi.org/10.1023/B:NHAZ.0000024895.48463.eb.

Benito, G., Rico, M., Sánchez-Moya, Y., Sopeña, A., Thorndycraft, V.R., Barriendos, M., 2010. The impact of late Holocene climatic variability and land use change on the flood hydrology of the Guadalentín River, Southeast Spain. Glob. Planet. Chang. 70, 53–63. https://doi.org/10.1016/j.gloplacha.2009.11.007.

Benito, G., Sanchez-Moya, Y., Medialdea, A., Barriendos, M., Calle, M., Rico, M., Sopeña, A., Machado, M.J., 2020b. Extreme floods in small mediterranean catchments: long-term response to climate variability and change. Water 2020 (12), 1008. https://doi.org/10.3390/w12041008.

Benito, G., Harden, T.M., O'Connor, J., 2020a. Quantitative Paleoflood hydrology. Treat. Geomorphol. 6 (22), 743–764. https://doi.org/10.1016/b978-0-12-409548-9.12495-9.

Blott, S.J., Pye, K., 2001. GRADISTAT: a grain size distribution and statistics package for the analysis of unconsolidated sediments. Earth Surf. Process. Landf. 26 (11), 1237–1248. https://doi.org/10.1002/esp.261.

Botero, B.A., Francés, F., 2006. AFINS Version 2.0-Análisis de Frecuencia de Extremos con Información Sistemática y No Sistemática. Research Group on Hydraulic and Hydrology. Department of Hydraulic Engineering and Environment, Politechnical University of Valencia. http://lluvia.dihma.upv.es/.

Botes, A., Henderson, J., Nakale, T., Nantanga, K., Schachtschneider, K., Seely, M., 2003. Ephemeral rivers and their development: testing an approach to basin management committees on the Kuiseb River, Namibia. Phys. Chem. Earth 28, 853–858. https://doi.org/10.1016/j.pce.2003.08.028.

Bowman, I., 1925. Desert Trails of Atacama. American Geographical Society, New York.

Bozkurt, D., Rondanelli, R., Garreaud, R., Arriagada, A., 2016. Impact of warmer eastern tropical pacific SST on the March 2015 Atacama floods. Mon. Weather Rev. 144 (11), 4441–4460. https://doi.org/10.1175/MWR-D-16-0041.1.

Cartigny, M.J.B., Ventra, D., Postma, G., van Den Berg, J.H., 2014. Morphodynamics and sedimentary structures of bedforms under supercritical-flow conditions: New insights from flume experiments. Sedimentology 61, 712–748. https://doi.org/10.1111/sed.12076.

Chakraborty, C., Bose, P.K., 1992. Ripple/dune to upper stage plane bed transition: some observations from the ancient record. Geol. J. 27, 349–359.

Chow, V., 2004. Applied Hydrology. McGraw-hill.

Cloete, G., Benito, G., Grodek, T., Porat, N., Enzel, Y., 2018. Analyses of the magnitude and frequency of a 400-year flood record in the Fish River Basin, Namibia. Geomorphology 320, 1–17. https://doi.org/10.1016/j.geomorph.2018.07.025.

Cloete, G., Benito, G., Grodek, T., Porat, N., Hoffman, J., Enzel, Y., 2022. Palaeoflood records to assist in design of civil infrastructure in ephemeral rivers with scarce hydrological data: Ugab River, Namibia. J. Hydrol. Reg. Stud. 44, 101263 https://doi.org/10.1016/j.ejrh.2022.101263.

Darwin, C., 1845. Journal of Researches into the Natural History and Geology of the Countries Visited during the Voyage of HMS Beagle Round the World, under the Command of Capt. Fitz Roy, R.N. John Murray, London.

De Martonne, E., 1935. Problème des régions arides sud-américaines. Ann. Géogr. 44, 1–27.

DGA, 2010. Análisis integrado de gestión en la cuenca del río Copiapó. Informe Final – Tomo I Resumen Ejecutivo. Dirección General de Aguas, Ministerio de Obras Públicas.

DOH, 2016. Caracterización y levantamiento de información debido a las crecidas aluvionales en la cuenca del rio Copiapó - Región de Atacama, para el temporal del 25 y 26 de marzo de 2015. Dirección Obras Hidráulicas, Ministerio de Obras Públicas, Chile.

Falabella, F., Uribe, M., Sanhueza, L., Aldunate, C., Hidalgo, J., 2017. Prehistoria en Chile: desde sus primeros habitantes hasta los Incas. Editorial Universitaria, Santiago de Chile, p. 737.

Fielding, C.R., 2006. Upper flow regime sheets, lenses and scour fills: extending the range of architectural elements for fluvial sediment bodies. Sediment. Geol. 190 (1–4), 227–240. https://doi.org/10.1016/j.sedgeo.2006.05.009.

Folk, R.L., Ward, W.C., 1957. Brazos River bar: a study in the significance of grain size parameters. J. Sediment. Petrol. 27, 3–26.

Fournier, J., Gallon, R., Paris, R., 2014. G2Sd: a new R package for the statistical analysis of unconsolidated sediments. Geomorphol. Relief Proc. Environn. 20(1), 73-78. http://geomorphologie.revues.org/10513.

Freund, M.B., Henley, B.J., Karoly, D.J., McGregor, H.V., Abram, N.J., Dommenget, D., 2019. Higher frequency of Central Pacific El Niño events in recent decades relative to past centuries. Nat. Geosci. 12 (6), 450–455. https://doi.org/10.1038/s41561-019-0353-3.

Godoy, E., Marquardt, C., Blanco, N., 2003. Carta Caldera, Región de Atacama. Servicio Nacional de Geología y Minería, Carta Geológica de Chile. Ser. Geol. Básica 76, 38.

Grodek, T., Benito, G., Botero, B.A., Jacoby, Y., Porat, N., Haviv, I., Cloete, G., Enzel, Y., 2013. The last millennium largest floods in the hyperarid Kuiseb River basin, Namib Desert. J. Quat. Sci. 28 (3), 258–270. https://doi.org/10.1002/jqs.2618.

Hogg, A.G., Hua, Q., Blackwell, P.G., Niu, M., Buck, C.E., Guilderson, T.P., Heaton, T.J., Palmer, J.G., Reimer, P.J., Reimer, R.W., Turney, C.S.M., Zimmerman, S.R., 2013. SHCal13 Southern Hemisphere calibration, 0–50,000 years cal BP. Radiocarbon 55 (4), 1889–1903. https://doi.org/10.2458/azu_js_rc.55.16783.

Houston, J., 2006a. Variability of precipitation in the Atacama Desert: its causes and hydrological impact. Int. J. Climatol. 26, 2181–2198. https://doi.org/10.1002/joc.1359.

Houston, J., 2006b. The great Atacama flood of 2001 and its implications for Andean hydrology. Hydrol. Process. 20, 591–610. https://doi.org/10.1002/hyp.5926.

Hydrologic Engineering Center, 2010. HEC-RAS 4.1, River Analysis System, Hydraulics Version 4.1. Reference Manual, (CPD-69). U.S. Army Corps of Engineers, Davis, p. 411.

IPCC, 2023. AR6 Synthesis Report: Climate Change 2023. Geneva, Switzerland, IPCC, p. 40.

Iribarren Anacona, P., Norton, K., Mackintosh, A., Escobar, F., Allen, S., Mazzorana, B., Schaefer, M., 2018. Dynamics of an outburst flood originating from a small and high-altitude glacier in the Arid Andes of Chile. Nat. Hazards 94, 93–119. https://doi.org/10.1007/s11069-018-3376-y.

Izquierdo, T., Abad, M., Larrondo, L., 2017. Paleohydrology of late Quaternary floods in the Atacama Desert and their paleoclimate implications. Geophys. Res. Abstr. 19, 10261.

Izquierdo, T., Rivera, A., Abad, M., 2019. Identification of Extraordinary Floods in the Late Holocene Fluvial Deposits of the Copiapó River (Southern Atacama Desert, Chile). INQUA, Dublin (Ireland).

Izquierdo, T., Bonnail, E., Abad, M., Días, M.I., Prudêncio, M.I., Marques, R., Rodríguez-Vidal, J., Ruiz, F., 2020. Pollution and potential risk assessment of flood sediments in the urban area of the mining Copiapó basin (Atacama Desert). J. S. Am. Earth Sci. 103, 102714 https://doi.org/10.1016/j.jsames.2020.102714.

Izquierdo, T., Abad, M., Gómez, Y., Gallardo, D., Rodríguez-Vidal, J., 2021. The March 2015 catastrophic flood event and its impacts in the city of Copiapó (southern Atacama Desert). An integrated analysis to mitigate future mudflow derived damages. J. S. Am. Earth Sci. 105, 102975 https://doi.org/10.1016/j.jsames.2020.102975.

Lang, J., Le Heron, D.P., Van den Berg, J.H., Winsemann, J., 2020. Bedforms and sedimentary structures related to supercritical flows in glacigenic settings. Sedimentology 68 (4), 1539–1579. https://doi.org/10.1111/sed.12776.

Liu, T., Greenbaumc, N., Baker, V.R., Ji, L., Onken, J., Weisheit, J., Porat, N., Rittenour, T., 2020. Paleoflood hydrology on the lower Green River, upper Colorado River Basin, USA: an example of a naturalist approach to flood-risk analysis. J. Hydrol. 580, 124337 https://doi.org/10.1016/j.jhydrol.2019.124337.

Lowe, D.R., 1975. Water escape Structures in coarse-grained sediments. Sedimentology 22, 157–204. https://doi.org/10.1111/j.1365-3091.1975.tb00290.x.
Mackenna, B.V., 1877. Ensayo histórico sobre el clima de Chile:(desde los tiempos prehistóricos hasta el gran temporal de julio de 1877). Imprenta del Mercurio, Santiago de Chile.
Macklin, M.G., Tooth, S., Brewer, P.A., Noble, P.L., Duller, G.A.T., 2010. Holocene flooding and river development in a Mediterranean steepland catchment: the Anapodaris Gorge, south Central Crete, Greece. Glob. Planet. Chang. 70, 35–52. https://doi.org/10.1016/j.gloplacha.2009.11.006.
Marquardt, C., Lavenu, A., Ortlieb, L., Godoy, E., Comte, D., 2004. Coastal neotectonics in Southern Central Andes: uplift and deformation of marine terraces in Northern Chile (27°S). Tectonophysics 394, 193–219. https://doi.org/10.1016/j.tecto.2004.07.059.
McKee, T.B., Doesken, N.J., Kleist, J., 1993. The Relationship of Drought Frequency and Duration to Time Scales. Preprints, Eighth Conference on Applied Climatology. American Meteorological Society, Anaheim, CA, pp. 179–184.
Meza, A.C., Muñoz, M.C., Whittaker, M.A.C., 1992. Historia de las catástrofes ocurridas en la Región de Atacama. Investigación y seminario para optar al Título de Profesor de Educación General Básica con mención en Ciencias Sociales y al Grado de Licenciado en Educación. Universidad de Atacama.
Miall, A.D., 1985. Architectural-element analysis: a new method of facies analysis applied to fluvial deposits. Earth Sci. Rev. 22 (4), 261–308. https://doi.org/10.1016/0012-8252(85)90001-7.
Miller, J.R., Walsh, D., Villarroel, L.F., 2019. Use of paleoflood deposits to determine the contribution of anthropogenic trace metals to alluvial sediments in the hyperarid Rio Loa Basin, Chile. Geosciences 9, 244. https://doi.org/10.3390/geosciences9060244.
Milly, P.C.D., Wetherald, R.T., Dunne, K.A., Delworth, T.L., 2002. Increasing risk of great floods in a changing climate. Nature 415, 514–517. https://doi.org/10.1038/415514a.
Morin, E., Grodek, T., Dahan, O., Benito, G., Kulls, C., Van Jacoby, Y., Langenhove, G., Seely, M., Enzel, Y., 2009. Flood routing and alluvial aquifer recharge along the ephemeral arid Kuiseb River, Namibia. J. Hydrol. 368, 262–275. https://doi.org/10.1016/j.jhydrol.2009.02.015.
Navarro, N., Abad, M., Bonnail, E., Izquierdo, T., 2021. The arid coastal wetlands of Northern Chile: towards an integrated management of highly threatened systems. J. Mar. Sci. Eng. 9, 948. https://doi.org/10.3390/jmse9090948.
Niemeyer, H., Cervellino, M., Castillo, G., 1997. Culturas prehistóricas de Copiapó. Gobierno Regional de Atacama, 282 pp.
Observatorio Económico Chile, 2015. Impacto Económico de los temporales que afectan el Norte del país, 8. BBVA Internal Report. https://www.bbvaresearch.com/wp-content/uploads/2015/04/Chile_temporales_20151.pdf (Accessed 11 May 2023).
Orellana, M., 2005. Chile en el siglo XVI: aborígenes y españoles. El proceso de aculturación, Librotecnia, 224 pp.
Ortega, C., Vargas, G., Rojas, M., Rutlant, J.A., Muñoz, P., Lange, C.B., Pantoja, S., Dezileau, L., Ortlieb, L., 2019. Extreme ENSO-driven torrential rainfalls at the southern edge of the Atacama Desert during the late Holocene and their projection into the 21th century. Glob. Planet. Chang. 175, 226–237. https://doi.org/10.1016/j.gloplacha.2019.02.011.
Ortlieb, L., 1995. Eventos El Niño y episodios lluviosos en el desierto de Atacama: el registro de los últimos dos siglos. Bull. Inst. Franç. étud. Andin. 24 (3), 519–537.
Ortlieb, L., Vargas, G., 2015. Hacia una historia de eventos lluviosos extremos en el sur del Desierto de Atacama, Norte Chico, a partir de fuentes documentales. XIV Congreso Geológico Chileno, La Serena (Chile).
Philippi, R.A., 1860. Viage al Desierto de Atacama hecho de orden del Gobierno de Chile en el verano 1853–54.
Quezada, J., González, G., Dunai, T., Jensen, A., Juez-Larré, J., 2007. Alzamiento litoral Pleistoceno del norte de Chile: edades 21Ne de la terraza costera más alta del área de Caldera-Bahía Inglesa. Rev. Geol. Chile 34, 81–96.
R Core Team, 2023. R: A Language and Environment for Statistical Computing. R Foundation for Statistical Computing, Vienna, Austria. URL. https://www.R-project.org/.
Sayago, C.M., 1874. Historia de Copiapó. Imp. de El Atacama (Copiapó). 450 p.
Schick, A.P., 1988. Hydrological aspects of floods in extreme arid environments. In: Baker, V.R., Kochel, R.C., Patton, P.C. (Eds.), Flood Geomorphology. Wiley, New York, pp. 189–203.
Schulte, L., Schillereff, D., Santisteban, J.I., 2019. Pluridisciplinary analysis and multi-archive reconstruction of paleofloods: societal demand, challenges and progress. Glob. Planet. Chang. 177, 225–238. https://doi.org/10.1016/j.gloplacha.2019.03.019.
Sparelli, I., Albertini, L., Izquierdo, T., Abad, M., Mozzi, P., Fontana, A., 2018. Geomorphological analysis of recent flash-flood events in the Atacama Desert using high-resolution UAV images. Geophys. Res. Abstr. 20. EGU2018-9225.
Stedinger, J.R., Cohn, T.A., 1986. Flood frequency analysis with historical and paleoflood information. Water Resour. Res. 22 (5), 785–793. https://doi.org/10.1029/WR022i005p00785.
Stuiver, M., Reimer, P.J., Reimer, R.W., 2013. Calib 7.0. Radiocarbon Calibration Program. http://calib.org/calib/download/calib704.zip.
Urrutia, R., Lanza, C., 1993. PCatástrofes en Chile. La Noria. 1541-1992, 405. https://bibliotecadigital.ciren.cl/handle/20.500.13082/18899.
Valdés-Pineda, R., Pizarro, R., García-Chevesich, P., Valdés, J.B., Olivares, C., Vera, M., Balocchi, F., Pérez, F., Vallejos, C., Fuentes, R., Abarza, A., Helwig, B., 2014. Water governance in Chile: availability, management and climate change. J. Hydrol. 519, 2538–2567. https://doi.org/10.1016/j.jhydrol.2014.04.016.
Valdés-Pineda, R., Cañón, J., Valdés, J.B., 2018. Multi-decadal 40- to 60-year cycles of precipitation variability in Chile (South America) and their relationship to the AMO and PDO signals. J. Hydrol. 556, 1153–1170. https://doi.org/10.1016/j.jhydrol.2017.01.031.
Vargas, G., Orlieb, L., Rutllant, J., 2000. Aluviones históricos en Antofagasta y su relación con eventos El Niño/Oscilación del Sur. Rev. Geol. Chile 27 (2), 157–176. https://doi.org/10.4067/S0716-02082000000200002.
Vargas, G., Rutllant, J., Ortlieb, L., 2006. ENSO tropical–extratropical climate teleconnections and mechanisms for Holocene debris flows along the hyperarid coast of western South America (17–24 S). Earth Planet. Sci. Lett. 249 (3–4), 467–483. https://doi.org/10.1016/j.epsl.2006.07.022.
Webb, R.H., Jarrett, R.D., 2002. One-dimensional estimation techniques for discharges of paleofloods and historical floods. In: House, P.K., Webb, R.H., Baker, V.R., Levish, D. R. (Eds.), Ancient Floods, Modern Hazards: Principles and Applications of Paleoflood Hydrology, Vol. 5, pp. 111–125. https://doi.org/10.1029/WS005p0111.
Wilhelm, B., Ballesteros Cánovas, J.A., Macdonald, N., Toonen, W.H., Baker, V., Barriendos, M., Benito, G., Brauer, A., Corella, J.P., Denniston, R., Glaser, R., Ionita, M., Kahle, M., Liu, T., Luetscher, M., Macklin, M., Mudelsee, M., Munoz, S., Schulte, L., St. George, S., Stoffel, M., Wetter, O., 2019. Interpreting historical, botanical, and geological evidence to aid preparations for future floods. Wiley Interdiscip. Rev. Water 6 (1), e1318. https://doi.org/10.1002/wat2.1318.